

Populations of close binaries in galaxies with recent bursts of starformation

S.B. Popov,
 (<http://xray.sai.msu.su/~polar/>)
 M.E. Prokhorov & V.M. Lipunov

Sternberg Astronomical Institute
 Moscow State University

Abstract

This paper is a continuation and development of our previous articles (Popov et al., 1997, 1998). We use “Scenario Machine” (Lipunov et al., 1996b) – the population synthesis simulator (for single binary systems calculations the program is available in WWW: <http://xray.sai.msu.su/sciwork/scenario.html> (Nazin et al., 1998) – to calculate evolution of populations of several types of X-ray sources during the first 20 Myrs after a starformation burst.

We examined the evolution of 12 types of X-ray sources in close binary systems (both with neutron stars and with black holes) for different parameters of the IMF – slopes: $\alpha = 1$, $\alpha = 1.35$ and $\alpha = 2.35$ and upper mass limits: $120 M_{\odot}$, $60 M_{\odot}$ and $40 M_{\odot}$. Results, especially for sources with black holes, are very sensitive to variations of the IMF, and it should be taken into account when fitting parameters of starformation bursts.

Results are applied to several regions of recent starformation in different galaxies: Tol 89, NGC 5253, NGC 3125, He 2-10, NGC 3049. Using known ages and total masses of starformation bursts (Shaerer et al., 1998) we calculate expected numbers of X-ray sources in close binaries for different parameters of the IMF. Usually, X-ray transient sources consisting of a neutron star and a main sequence star are most abundant, but for very small ages of bursts (less than ≈ 4 Myrs) sources with black holes can become more abundant.

1 Introduction.

Theory of stellar evolution and one of the strongest tools of that theory – population synthesis – are now rapidly developing branches of astrophysics. Very often only the evolution of single stars is modelled, but it is well known that about 50% of all stars are members of binary systems, and a lot of different astrophysical objects are products of the evolution of binary stars. We argue, that often it is necessary to take into account the evolution of close binaries while using the population synthesis in order to avoid serious errors.

Initially this work was stimulated by the article Contini et al. (1995), where the authors suggested an unusual form of the initial mass function (IMF) for the explanation of the observed properties of the galaxy Mrk 712. They suggested the “flat” IMF with the exponent $\alpha = 1$ instead of the Salpeter’s value $\alpha = 2.35$. Contini et al. (1995) didn’t take into account binary systems, so no words about the influence of such IMF on the populations of close binary stars could be said. Later Shaerer (1996) showed that the observations could be explained without the IMF with $\alpha = 1$. Here we try to determine the influence of the variations of the IMF on the evolution of compact binaries and apply our results to seven regions of starformation (Shaerer et al., 1998, hereafter SCK98).

Previously (Lipunov et al., 1996a) we used the “Scenario Machine” for calculations of populations of X-ray sources after a burst of starformation at the Galactic center. Here, as before in Popov et al. (1997, 1998), we model a general situation — we make calculations for a typical starformation burst. We show results on twelve types of binary sources with significant X-ray luminosity for three values of the upper mass limit for three values of α .

2 Model.

Monte-Carlo method for statistical simulations of binary evolution was originally proposed by Kornilov & Lipunov (1983a,b) for massive binaries and developed later by Lipunov & Postnov (1987) for low-massive binaries. Dewey & Cordes (1987) applied an analogous method for analysis of radio pulsar statistics, and de Kool (1992) investigated by the Monte-Carlo method the formation of the galactic cataclysmic variables (see the review in van den Heuvel 1994).

Monte-Carlo simulations of binary star evolution allows one to investigate the evolution of a large ensemble of binaries and to estimate the number of binaries at different evolutionary stages. Inevitable simplifications in the analytical description of the binary evolution that we allow in our extensive numerical calculations, make those numbers approximate to a factor of 2-3. However, the inaccuracy of direct calculations giving the numbers of different binary types in the Galaxy (see e.g. Iben & Tutukov 1984, van den Heuvel 1994) seems to be comparable to what follows from the simplifications in the binary evolution treatment.

In our analysis of binary evolution, we use the “Scenario Machine”, a computer code, that incorporates current scenarios of binary evolution and takes into account the influence of magnetic field of compact objects on their observational appearance. A detailed description of the computational techniques and input assumptions is summarized elsewhere (Lipunov et al. 1996b; see also: <http://xray.sai.msu.su/~mystery/articles/review/>), and here we briefly list only principal parameters and initial distributions.

We trace the evolution of binary systems during the first 20 Myrs after their formation in a starformation burst. Obviously, only stars that are massive enough (with masses $\geq 8 - 10 M_{\odot}$) can evolve off the main sequence during the time as short as this to yield compact remnants: neutron stars (NSs) and black holes (BHs). Therefore we consider only massive binaries, i.e. those having the mass of the primary (more massive) component in the range of $10 - 120 M_{\odot}$.

The distribution in orbital separations is taken as deduced from observations:

$$f(\log a) = \text{const}, \quad \max \{10 R_{\odot}, \text{Roche Lobe } M(M_1)\} < \log a < 10^7 R_{\odot}. \quad (1)$$

We assume that a NS with a mass of $1.4 M_{\odot}$ is formed as a result of the collapse of a star, whose core mass prior to collapse was $M_* \sim (2.5 - 35) M_{\odot}$. This corresponds to an initial mass range $\sim (10 - 60) M_{\odot}$, taking into account that a massive star can lose more than $\sim (10 - 20)\%$ of its initial mass during the evolution with a strong stellar wind.

The most massive stars are assumed to collapse into a BH once their mass before the collapse is $M > M_{cr} = 35 M_{\odot}$ (which would correspond to an initial mass of the ZAMS star as high as $\sim 60 M_{\odot}$ since a substantial mass loss due to a strong stellar wind occurs for the most massive stars). The BH mass is calculated as $M_{bh} = k_{bh} M_{cr}$, where the parameter k_{bh} is taken to be 0.7.

The mass limit for NS (the Oppenheimer-Volkoff limit) is taken to be $M_{OV} = 2.5 M_{\odot}$, which corresponds to a hard equation of state of the NS matter.

We made calculations for several values of the coefficient α :

$$\frac{dN}{dM} \propto M^{-\alpha} \quad (2)$$

We calculated 10^7 systems in every run of the program. Then the results were normalized to the total mass of binary stars in the starformation burst. We also used different values of the upper mass limit.

We took into account that the collapse of a massive star into a NS can be asymmetrical, so that an additional kick velocity, v_{kick} , presumably randomly oriented in space, should be imparted to the newborn compact object. We used the velocity distribution in the form obtained by Lyne & Lorimer (1994) with the characteristic value 200 km/s (twice less than in Lyne & Lorimer (1994), see Lipunov et al. (1996c)).

3 Results.

On the figures we show the results of our calculations. On all graphs on the X-axis we show the time after the starformation burst in Myrs, on the Y- axis — number of the sources of the selected type that exist at the particular moment (not the birth rate of the sources!).

On figures 1-3 we show our calculations for X-ray sources of 12 different types for different parameters of the IMF.

- Figure 1 — $\alpha = 1$,
- Figure 2 — $\alpha = 1.35$,
- Figure 3 — $\alpha = 2.35$.

For upper mass limits:

- $120M_{\odot}$ — solid lines,
- $60M_{\odot}$ — dashed lines,
- $40M_{\odot}$ — dotted lines.

The calculated numbers were normalized for $1 \cdot 10^6 M_{\odot}$ in binary stars. We show on the figures 1-3 and in tables 1-9 only systems with the luminosity of compact object greater than 10^{33} erg/s (it should be mainly X-ray luminosity).

Curves were not smoothed so all fluctuations of statistical nature are presented. We calculated 10^7 binary systems in every run, and then the results were normalized.

We used the “flat” mass ratio function, i.e. binary systems with any mass ratio appear with the same probability. The results can be renormalized to any other form of the mass ratio function.

4 Application of our calculations

We apply our results to seven regions of recent starformation. Ages, total masses and some other characteristics were taken from SCK98 (we used total masses determined for Salpeter’s IMF even for the IMFs with different parameters, which is a simplification). As far as for several regions ages are uncertain, we made calculations for two values of the age, marked in SCK98.

Results are presented in tables 1-9 (regions NGC3125A and NGC3125B have similar ages and total masses). We made an assumption, that binaries contain 50% of the total mass of the starburst. Numbers were rounded off to the nearest integer (i.e. n sources means, that calculated number was between $n-0.5$ and $n+0.5$).

5 Discussion and conclusions

Different types of close binaries show different sensitivity to variations of the IMF. When we replace $\alpha = 2.35$ by $\alpha = 1$ the numbers of all sources increase. Systems with BHs are more sensitive to such variations.

When one try to vary the upper mass limit, another situation appear. In some cases (especially for $\alpha = 2.35$) systems with NSs show little differences for different values of the upper mass limit, while systems with BHs become significantly less (or more) abundant for different upper masses. Luckily, X-ray transients, which are the most numerous systems in our calculations, show significant sensitivity to variations of the upper mass limit. But of course due to their transient nature it is difficult to use them to detect small variations in the IMF. If it is possible to distinguish systems with BH, it is much better to use them to test the IMF.

The results of our calculations can be easily used to estimate the number of X-ray sources for different parameters of the IMF if the total mass of stars and age of a starburst are known (in (Popov et al., 1997, 1998) analytical approximations for source numbers were given). And we estimate numbers of different sources for several regions of recent starformation (tables 1-9).

In this poster we also tried to show, that, as expected, populations of close binaries are very sensitive to the variations of the IMF. One must be careful, when trying to fit the observed data for single stars with variations of the IMF. And, vice versa, using detailed observations of X-ray sources, one can try to estimate parameters of the IMF, and test results, obtained from single stars population.

6 Acknowledgements

We want to thank Dr. K.A. Postnov for discussions and G.V. Lipunova and Dr. I.E. Panchenko for technical assistance.

This work was supported by the grants: NTP “Astronomy” 1.4.2.3., NTP “Astronomy” 1.4.4.1 and “Universities of Russia” N5559.

We are also thankful to the organizers of the conference for support and hospitality.

References

- [1] Contini, T., Davoust, E., & Consideré, S., 1995, *A & A* **303**, 440
- [2] de Kool, M. 1992, *A&A*, **261**, 188
- [3] Dewey, R.J. & Cordes, J.M. 1987, *ApJ*, **321**, 780
- [4] Iben, I., Jr. & Tutukov, A.V. 1984, *ApJ*, **284**, 719
- [5] Kornilov, V.G. & Lipunov, V.M. 1983b, *AZh*, **60**, 574
- [6] Kornilov, V.G. & Lipunov, V.M. 1983a, *AZh*, **60**, 284
- [7] Lipunov, V.M., Ozernoy, L.M., Popov, S.B., Postnov, K.A. & Prokhorov, M.E., 1996a, *ApJ* **466**, 234
- [8] Lipunov, V.M., Postnov, K.A. & Prokhorov, M.E., 1996b, *Astroph. and Space Phys. Rev.* **9**, part 4
- [9] Lipunov, V.M., Postnov, K.A., & Prokhorov, M.E., 1996c, *A & A* **310**, 489
- [10] Lipunov, V.M. & Postnov, K.A. 1987, *Ap.& Sp.Sci.* **145**, 1
- [11] Lyne, A.G., & Lorimer, D.R., 1994, *Nature* **369**, 127
- [12] Nazin, , S.N., Lipunov, V.M., Panchenko, I.E., Postnov, K.A., Prokhorov, M.E. & Popov, S.B., 1998, *Grav. & Cosmology*, **4**, suppl. “Cosmoparticle Physics” part.1, 150 (astro-ph 9605184)
- [13] Popov, S.B., Lipunov, V.M., Prokhorov, M.E., & Postnov, K.A., 1997, astro-ph/9711352
- [14] Popov, S.B., Lipunov, V.M., Prokhorov, M.E., & Postnov, K.A., 1998, *AZh*, **75**, 35 (astro-ph/9812416)
- [15] Schaefer, D., 1996, *ApJ* **467**, L17
- [16] Schaefer, D., Contini, T., & Kunth, D., 1998, *A&A* **341**, 399 (astro-ph/9809015) (SCK98)
- [17] Schaller, G., Schaefer, D., Meynet, G., & Maeder, A., 1992, *A & A Supp.* **96**, 269
- [18] van den Heuvel, E.P.J., 1994, in ‘Interacting Binaries’, Eds. Shore, S.N., Livio, M., & van den Heuvel, E.P.J., Berlin, Springer, 442

TWELVE TYPES OF X-RAY SOURCES

BH+N2 — A BH with a He-core Star (Giant)

NA+N1 — An Accreting NS with a Main Sequence Star (Be-transient)

BH+WR — A BH with a Wolf-Rayet Star

BH+N1 — A BH with a Main Sequence Star

BH+N3G — A BH with a Roche-lobe filling star, when the binary loses angular momentum by grav. radiation

NA+N3 — An Accreting NSt with a Roche-lobe filling star (fast mass transfer from the more massive star)

NA+WR — An Accreting NS with a Wolf-Rayet Star

BH+N3E — A BH with a Roche-lobe filling star (nuclear evolution time scale)

NA+N3G — An Accreting NS with a Roche-lobe filling star, when the binary loses angular momentum due to gravitational radiation

NA+N3M — An Accreting NS with a Roche-lobe filling star, when the binary loses angular momentum due to magnetic wind

NA+N2 — An Accreting NS with a He-core Star (Giant)

NA+N3E — An Accreting NS with a Roche-lobe filling star (nuclear evolution time scale)

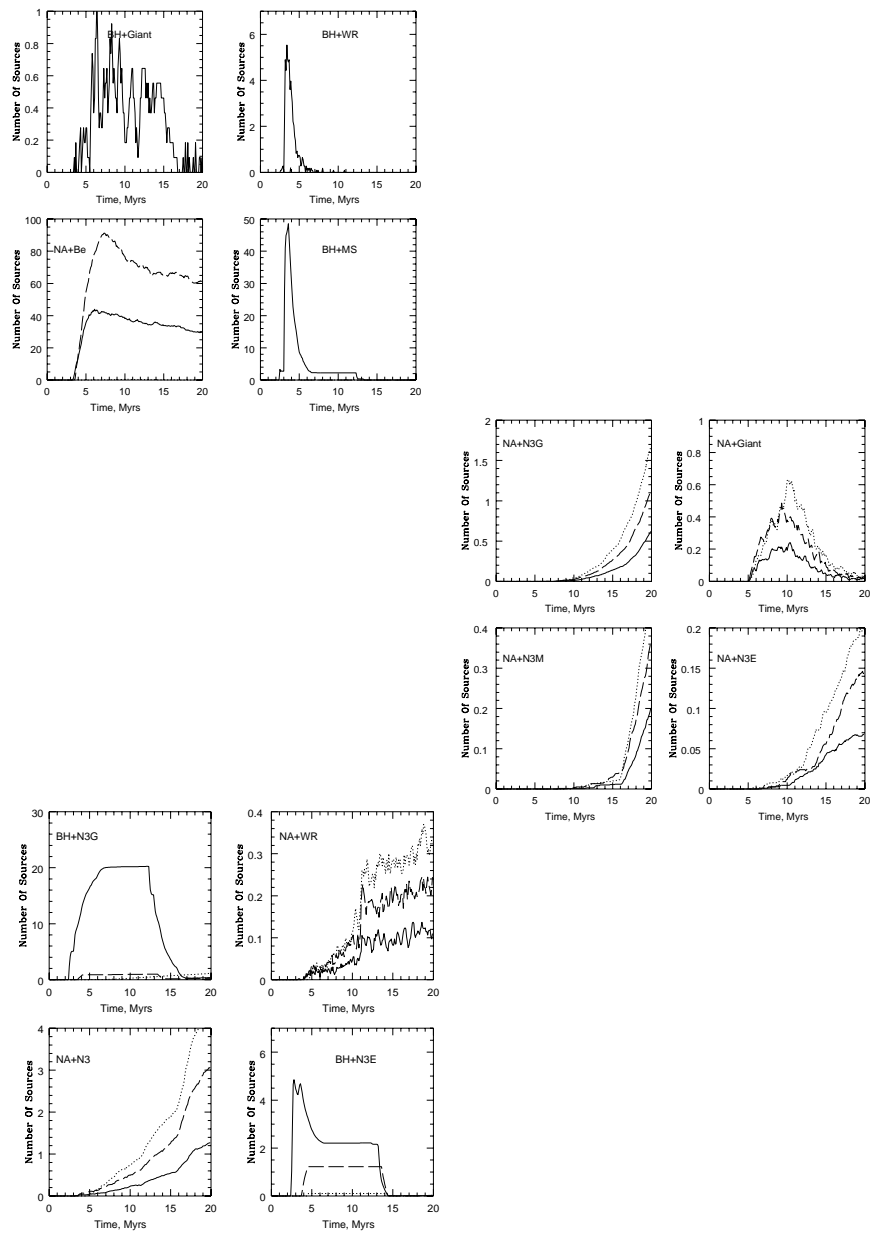


Figure 1

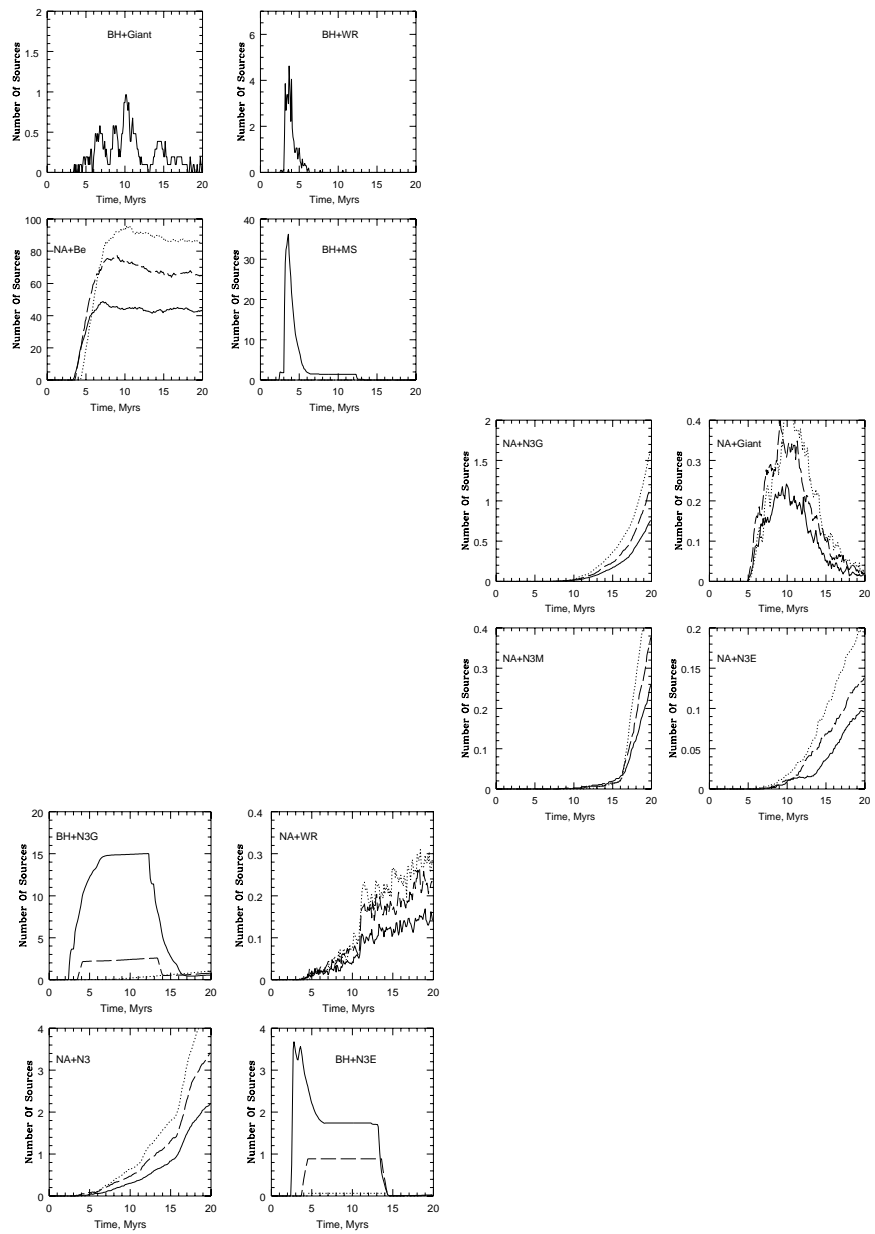


Figure 2

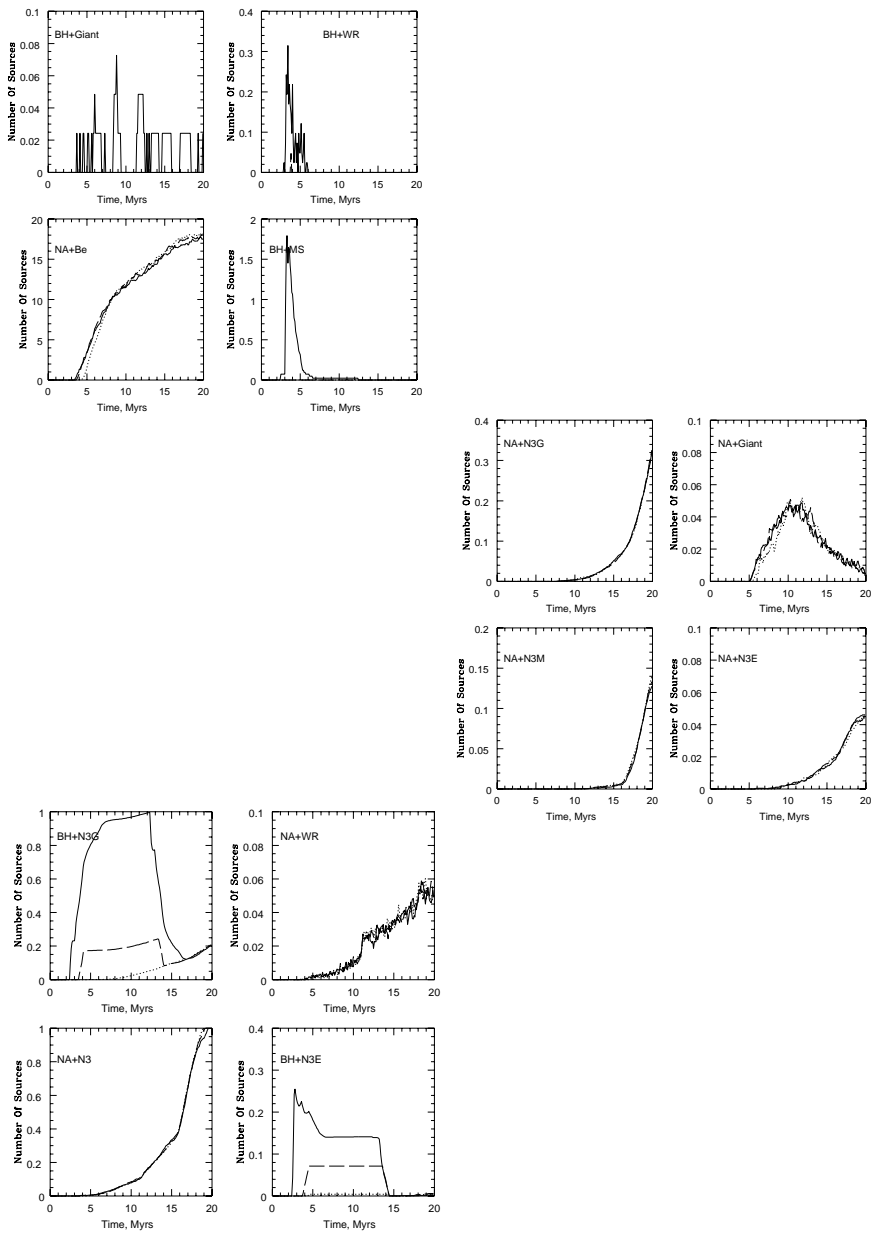


Figure 3

Table 1: He 2-10; age 5.5 Myrs; total mass $10^{6.8} M_{\odot}$

Slope	2.35	2.35	2.35	1.35	1.35	1.35	1.01	1.01	1.01
Up.mas.	120	60	40	120	60	40	120	60	40
bh+n1	0	0	0	16	0	0	28	0	0
bh+n2	0	0	0	0	0	0	0	0	0
bh+n3e	1	0	0	9	4	0	12	6	1
bh+n3g	4	1	0	62	10	0	84	4	0
bh+wr	0	0	0	1	0	0	3	0	0
na+n1	24	22	15	187	241	165	190	321	221
na+n3	0	0	0	0	0	0	0	1	0
na+wr	0	0	0	0	0	0	0	0	0
na+n3m	0	0	0	0	0	0	0	0	0
na+n3e	0	0	0	0	0	0	0	0	0
na+n3g	0	0	0	0	0	0	0	0	0
na+n2	0	0	0	0	0	0	0	0	0

Table 2: He 2-10; age 6.0 Myrs; total mass $10^{6.8} M_{\odot}$

Slope	2.35	2.35	2.35	1.35	1.35	1.35	1.01	1.01	1.01
Up.mas.	120	60	40	120	60	40	120	60	40
bh+n1	0	0	0	9	0	0	17	0	0
bh+n2	0	0	0	1	0	0	2	0	0
bh+n3e	1	0	0	9	4	0	11	6	1
bh+n3g	4	1	0	65	11	0	88	4	0
bh+wr	0	0	0	0	0	0	0	0	0
na+n1	29	30	22	198	283	233	202	367	322
na+n3	0	0	0	0	1	1	0	1	1
na+wr	0	0	0	0	0	0	0	0	0
na+n3m	0	0	0	0	0	0	0	0	0
na+n3e	0	0	0	0	0	0	0	0	0
na+n3g	0	0	0	0	0	0	0	0	0
na+n2	0	0	0	0	1	0	0	1	1

Table 3: NGC3125A, B; age 4.5 Myrs; total mass $10^{6.1} M_{\odot}$

Slope	2.35	2.35	2.35	1.35	1.35	1.35	1.01	1.01	1.01
Up.mas.	120	60	40	120	60	40	120	60	40
bh+n1	1	0	0	11	0	0	16	0	0
bh+n2	0	0	0	0	0	0	0	0	0
bh+n3e	0	0	0	2	1	0	3	1	0
bh+n3g	1	0	0	11	2	0	14	1	0
bh+wr	0	0	0	1	0	0	1	0	0
na+n1	2	2	0	21	24	5	24	33	6
na+n3	0	0	0	0	0	0	0	0	0
na+wr	0	0	0	0	0	0	0	0	0
na+n3m	0	0	0	0	0	0	0	0	0
na+n3e	0	0	0	0	0	0	0	0	0
na+n3g	0	0	0	0	0	0	0	0	0
na+n2	0	0	0	0	0	0	0	0	0

Table 4: NGC3125A, B; age 5.0 Myrs; total mass $10^{6.1} M_{\odot}$

Slope	2.35	2.35	2.35	1.35	1.35	1.35	1.01	1.01	1.01
Up.mas.	120	60	40	120	60	40	120	60	40
bh+n1	0	0	0	7	0	0	8	0	0
bh+n2	0	0	0	0	0	0	0	0	0
bh+n3e	0	0	0	2	1	0	3	1	0
bh+n3g	1	0	0	12	2	0	16	1	0
bh+wr	0	0	0	1	0	0	1	0	0
na+n1	3	3	1	29	36	18	34	52	25
na+n3	0	0	0	0	0	0	0	0	0
na+wr	0	0	0	0	0	0	0	0	0
na+n3m	0	0	0	0	0	0	0	0	0
na+n3e	0	0	0	0	0	0	0	0	0
na+n3g	0	0	0	0	0	0	0	0	0
na+n2	0	0	0	0	0	0	0	0	0

Table 5: NGC5253A; age 3.0 Myrs; total mass $10^{6.6} M_{\odot}$

Slope	2.35	2.35	2.35	1.35	1.35	1.35	1.01	1.01	1.01
Up.mas.	120	60	40	120	60	40	120	60	40
bh+n1	0	0	0	5	0	0	8	0	0
bh+n2	0	0	0	0	0	0	0	0	0
bh+n3e	1	0	0	10	0	0	13	0	0
bh+n3g	1	0	0	11	0	0	15	0	0
bh+wr	0	0	0	0	0	0	0	0	0
na+n1	0	0	0	0	0	0	0	0	0
na+n3	0	0	0	0	0	0	0	0	0
na+wr	0	0	0	0	0	0	0	0	0
na+n3m	0	0	0	0	0	0	0	0	0
na+n3e	0	0	0	0	0	0	0	0	0
na+n3g	0	0	0	0	0	0	0	0	0
na+n2	0	0	0	0	0	0	0	0	0

Table 6: NGC5253B; age 5.0 Myrs; total mass $10^{6.6} M_{\odot}$

Slope	2.35	2.35	2.35	1.35	1.35	1.35	1.01	1.01	1.01
Up.mas.	120	60	40	120	60	40	120	60	40
bh+n1	1	0	0	21	0	0	26	0	0
bh+n2	0	0	0	1	0	0	1	0	0
bh+n3e	1	0	0	7	3	0	8	4	0
bh+n3g	2	1	0	36	7	0	49	3	0
bh+wr	0	0	0	3	0	0	2	0	0
na+n1	11	10	5	92	112	58	106	163	80
na+n3	0	0	0	0	0	0	0	0	0
na+wr	0	0	0	0	0	0	0	0	0
na+n3m	0	0	0	0	0	0	0	0	0
na+n3e	0	0	0	0	0	0	0	0	0
na+n3g	0	0	0	0	0	0	0	0	0
na+n2	0	0	0	0	0	0	0	0	0

Table 7: Tol 89; age 4.5 Myrs; total mass $10^{5.7} M_{\odot}$

Slope	2.35	2.35	2.35	1.35	1.35	1.35	1.01	1.01	1.01
Up.mas.	120	60	40	120	60	40	120	60	40
bh+n1	0	0	0	4	0	0	6	0	0
bh+n2	0	0	0	0	0	0	0	0	0
bh+n3e	0	0	0	1	0	0	1	0	0
bh+n3g	0	0	0	4	1	0	6	0	0
bh+wr	0	0	0	0	0	0	1	0	0
na+n1	1	1	0	9	9	2	10	13	2
na+n3	0	0	0	0	0	0	0	0	0
na+wr	0	0	0	0	0	0	0	0	0
na+n3m	0	0	0	0	0	0	0	0	0
na+n3e	0	0	0	0	0	0	0	0	0
na+n3g	0	0	0	0	0	0	0	0	0
na+n2	0	0	0	0	0	0	0	0	0

Table 8: Tol 89; age 5.0 Myrs; total mass $10^{5.7} M_{\odot}$

Slope	2.35	2.35	2.35	1.35	1.35	1.35	1.01	1.01	1.01
Up.mas.	120	60	40	120	60	40	120	60	40
bh+n1	0	0	0	3	0	0	3	0	0
bh+n2	0	0	0	0	0	0	0	0	0
bh+n3e	0	0	0	1	0	0	1	0	0
bh+n3g	0	0	0	5	1	0	6	0	0
bh+wr	0	0	0	0	0	0	0	0	0
na+n1	1	1	1	12	14	7	13	21	10
na+n3	0	0	0	0	0	0	0	0	0
na+wr	0	0	0	0	0	0	0	0	0
na+n3m	0	0	0	0	0	0	0	0	0
na+n3e	0	0	0	0	0	0	0	0	0
na+n3g	0	0	0	0	0	0	0	0	0
na+n2	0	0	0	0	0	0	0	0	0

Table 9: NGC3049; age 5.5 Myrs; total mass $10^{6.4} M_{\odot}$

Slope	2.35	2.35	2.35	1.35	1.35	1.35	1.01	1.01	1.01
Up.mas.	120	60	40	120	60	40	120	60	40
bh+n1	0	0	0	7	0	0	11	0	0
bh+n2	0	0	0	0	0	0	0	0	0
bh+n3e	0	0	0	4	2	0	5	2	0
bh+n3g	2	0	0	24	4	0	33	2	0
bh+wr	0	0	0	1	0	0	1	0	0
na+n1	9	9	6	74	96	66	76	128	88
na+n3	0	0	0	0	0	0	0	0	0
na+wr	0	0	0	0	0	0	0	0	0
na+n3m	0	0	0	0	0	0	0	0	0
na+n3e	0	0	0	0	0	0	0	0	0
na+n3g	0	0	0	0	0	0	0	0	0
na+n2	0	0	0	0	0	0	0	0	0